remote sensing

MDPI

Article

Utilizing the Google Earth Engine for Agricultural Drought Conditions and Hazard Assessment Using Drought Indices in the Najd Region, Sultanate of Oman

Mohammed S. Al Nadabi [1], Paola D'Antonio [2], Costanza Fiorentino [2,*], Antonio Scopa [2], Eltaher M. Shams [3] and Mohamed E. Fadl [4]

[1] Department of Geographic Information Systems and Remote Sensing, Directorate General of Planning, Ministry of Agriculture, Fisheries and Water Resources, Muscat 100, Oman; mohammed.alnadabi@mafwr.gov.om
[2] School of Agricultural, Forest, Food, and Environmental Sciences (SAFE), University of Basilicata, Via dell'Ateneo Lucano 10, 85100 Potenza, Italy; paola.dantonio@unibas.it (P.D.)
[3] Geography and GIS Department, Faculty of Arts, Assiut University, Assiut 71526, Egypt; geomatic954@gmail.com
[4] Division of Scientific Training and Continuous Studies, National Authority for Remote Sensing and Space Sciences (NARSS), Cairo 11769, Egypt; madham@narss.sci.eg
* Correspondence: costanza.fiorentino@unibas.it

Abstract: Accurately evaluating drought and its effects on the natural environment is difficult in regions with limited climate monitoring stations, particularly in the hyper-arid region of the Sultanate of Oman. Rising global temperatures and increasing incidences of insufficient precipitation have turned drought into a major natural disaster worldwide. In Oman, drought constitutes a major threat to food security. In this study, drought indices (DIs), such as temperature condition index (TCI), vegetation condition index (VCI), and vegetation health index (VHI), which integrate data on drought streamflow, were applied using moderate resolution imaging spectroradiometer (MODIS) data and the Google Earth Engine (GEE) platform to monitor agricultural drought and assess the drought risks using the drought hazard index (DHI) during the period of 2001–2023. This approach allowed us to explore the spatial and temporal complexities of drought patterns in the Najd region. As a result, the detailed analysis of the TCI values exhibited temporal variations over the study period, with notable minimum values observed in specific years (2001, 2005, 2009, 2010, 2014, 2015, 2016, 2017, 2019, 2020, and 2021), and there was a discernible trend of increasing temperatures from 2014 to 2023 compared to earlier years. According to the VCI index, several years, including 2001, 2003, 2006, 2008, 2009, 2013, 2015, 2016, 2017, 2018, 2020, 2021, 2022, and 2023, were characterized by mild drought conditions. Except for 2005 and 2007, all studied years were classified as moderate drought years based on the VHI index. The Pearson correlation coefficient analysis (PCA) was utilized to observe the correlation between DIs, and a high positive correlation between VHI and VCI (0.829, $p < 0.01$) was found. Based on DHI index spatial analysis, the northern regions of the study area faced the most severe drought hazards, with severity gradually diminishing towards the south and east, and approximately 44% of the total area fell under moderate drought risk, while the remaining 56% was classified as facing very severe drought risk. This study emphasizes the importance of continued monitoring, proactive measures, and effective adaptation strategies to address the heightened risk of drought and its impacts on local ecosystems and communities.

Keywords: GEE; drought assessment; drought indices; drought hazard; MODIS

Citation: Al Nadabi, M.S.; D'Antonio, P.; Fiorentino, C.; Scopa, A.; Shams, E.M.; Fadl, M.E. Utilizing the Google Earth Engine for Agricultural Drought Conditions and Hazard Assessment Using Drought Indices in the Najd Region, Sultanate of Oman. *Remote Sens.* **2024**, *16*, 2960. https://doi.org/10.3390/rs16162960

Academic Editor: Gabriel Senay

Received: 25 June 2024
Revised: 5 August 2024
Accepted: 8 August 2024
Published: 12 August 2024

1. Introduction

Monitoring and evaluating the severity, frequency, duration, and spread of agricultural droughts is difficult due to their complex nature, particularly in hyper-arid regions

where there is a lack of data. Drought is a frequent natural disaster in arid and semi-arid lands, causing a range of environmental and socio-economic consequences [1]. Drought is a significant hydrometeorological phenomenon with far-reaching impacts on social and economic stability, second only to floods. Thus, effective mitigation and adaptation strategies are crucial for managing the risks associated with drought and reducing its detrimental effects [2]. Drought can be classified into different types based on the sectors affected, such as meteorological, hydrological, agricultural, and socio-economic droughts. Meteorological drought refers to a prolonged duration of below-average precipitation, meaning there is a significant precipitation deficit compared to the region's typical average precipitation; this type of drought is often the precursor to other forms of drought, as the lack of rainfall can lead to reduced water availability, impacting water bodies, agriculture, and socio-economic conditions [3]. Agricultural drought is distinguished by insufficient soil moisture levels, which fall below the threshold required for crop yield and vegetation health, impacting agricultural productivity and food supply [4]. Previous studies have primarily examined drought duration, severity, and frequency without specifically exploring the timing of droughts, including their onset and end, as well as the transitional phases, which are crucial for agricultural productivity [5,6]. A study of drought in Sichuan Province, China (1961–2016) [7] revealed a drying trend in the east and a wetting trend in the northwest, with extreme drought events becoming more frequent. The 3-month standardized precipitation index (SPI3) was identified as a strong short-term predictor of soil moisture drought, and the significant correlations with the Southern Oscillation Index (SOI) suggest that large-scale atmospheric patterns influence local drought conditions. Over the past decades, advances in remote sensing technology have greatly enhanced the ability to obtain global information on agricultural drought; these improvements have been driven by developments in satellite technology, data processing algorithms, and the integration of multiple sensor types [8]. Various methods have been devised to monitor and statistically characterize droughts; these include the creation of standardized and unstandardized drought indices utilized across meteorology, hydrology, and agricultural drought. Conventional methods for evaluating and monitoring drought rely on in-situ precipitation data, which often suffer from inaccuracies and limitations in both temporal and spatial coverage [9]. Droughts in Oman significantly affect the socio-economic environment and the human natural system, necessitating coordinated efforts in water management, agricultural practices, and policy implementation to mitigate their impacts. Oman, with its hyper-arid regions, such as the Najd area, faces severe challenges due to water scarcity, which affects agricultural productivity and food supply. Traditional methods of drought monitoring, which rely heavily on in-situ precipitation data, often suffer from inaccuracies and limitations in both temporal and spatial coverage; this is especially problematic in arid regions where weather stations may be sparse, and precipitation events can be highly localized and infrequent [10].

Remote sensing (RS) is a transformative technology that provides extensive data for environmental monitoring [11], including agricultural drought assessment in arid regions such as Oman, and addresses the critical challenge of data scarcity by offering continuous, comprehensive, and high-resolution data across both spatial and temporal resolution [7,12]. However, advancements in RS and earth observation technologies, such as MODIS imagery toward the end of the 20th century, have revolutionized agricultural drought monitoring methods [13].

Drought assessment relies on a variety of indices to derive different aspects of drought conditions, while indices such as VCI, TCI, and VHI are valuable tools, each focuses on specific aspects of drought, thereby addressing distinct types of droughts, such as agricultural, meteorological, or hydrological drought. VCI, TCI, and VHI are primarily vegetation indices and are integral to a multifaceted drought monitoring approach. By combining these indices with others that focus on precipitation (meteorological) and streamflow (hydrological), a more comprehensive understanding of drought can be achieved [14]. A global shift from a crisis management approach to a risk management approach in drought management has been strongly advocated. A key component of effective drought man-

agement is reliable drought risk assessment, as it elucidates the relationship between the hazard and society [15]. He et al. (2011) [16] conducted an analysis of agricultural drought hazard focusing on three primary crops (wheat, corn, and rice) using the standardized precipitation index (SPI); their results revealed that the eastern regions of China exhibited a higher hazard area compared to the western part in terms of agricultural drought risk.

The advent of cloud-based geospatial data monitoring platforms such as GEE has revolutionized the field of hydrometeorological applications. GEE leverages the power of cloud computing to access, process, and analyze vast amounts of satellite-based datasets, providing valuable insights into environmental conditions and changes, and GEE has greatly improved drought time series analysis capabilities, depending on large volumes of freely available satellite images and powerful image processing capabilities [17]. Assessing disaster risk due to drought involves a detailed analysis of hazard-forming factors, such as unusually low precipitation, drought intensity, occurrence probability, and duration. By integrating these factors into a comprehensive risk assessment framework using MODIS satellite images and the GEE platform, researchers and policymakers can better understand and mitigate the impacts of drought. Effective drought hazard assessments are crucial for safeguarding water resources, agricultural productivity, and overall socio-economic stability in affected regions [18].

Aksoy et al. (2019) [19] conducted a comprehensive analysis of drought conditions in Turkey from February 2000 to January 2019 using MODIS satellite data within the GEE platform, and in this study, drought, a frequently observed natural hazard resulting from precipitation deficit and increased evapotranspiration due to high temperatures, poses significant challenges to agricultural, water resource, and environmental management. RS indices, such as VHI, normalized multiband drought index (NMDI), and normalized difference drought index (NDDI), were utilized to assess the spatio-temporal distribution of drought severity across the country. Khan and Gilani, (2021) [20] provide a comprehensive analysis of drought conditions by utilizing a range of climatological and hydrological indices to assess the accumulative effects of various variables over time. This study focused on different types of droughts, agricultural, hydrological, and meteorological, by computing and analyzing specific indices, such as VCI, TCI, soil moisture condition index (SMCI), and precipitation condition index (PCI). This study identified specific years when these indices pointed to severe and extreme dryness conditions, providing a timeline of significant drought events using a dashboard created in the GEE platform. Ejaz et al. (2023) [21] demonstrate the efficacy of RS techniques in monitoring drought conditions in the hyper-arid region of the Kingdom of Saudi Arabia (KSA), where climatic observations are limited due to the sparsely distributed in-situ stations, and by leveraging multi-temporal satellite data from Landsat 7 (ETM+) and Landsat 8 (OLI/TIRS), processed through the GEE platform. The study computed DIs, including VCI, TCI, and VHI; these indices were compared against the standardized precipitation evapotranspiration index (SPEI), a conventional meteorological drought index, for the period from 2001 to 2020. Sazib et al. (2018) [22] demonstrate the substantial value of integrating advanced web-based tools based on soil moisture datasets into widely accessible platforms, such as GEE, thereby improving the monitoring and management of agricultural drought conditions on a global scale and developing user-friendly web-based tools to significantly enhance the ability to monitor agricultural drought.

Using Remote Sensing (RS), Geographic Information System (GIS), and the Google Earth Engine (GEE) platform, this study aims to characterize the spatiotemporal patterns of agricultural drought conditions in the Najd region from 2001 to 2023 by employing drought indices such as the vegetation condition index (VCI), temperature condition index (TCI), and vegetation health index (VHI) with MODIS satellite datasets. The study compares the reliability of these indices through principal component (PC) analysis. Additionally, it assesses the drought hazard in the region to provide a comprehensive evaluation of drought conditions and their impacts.

This study provides a comprehensive multi-assessment of agricultural drought characteristics in Oman and an effective method to monitor drought processes and mitigate their effects in this region that suffers from water scarcity.

2. Materials and Methods

2.1. Description of the Investigated Area

The study area located at Dhofar Governorate, southern Oman, known as the Najd region, covers approximately 88,000 km^2. Its boundaries are defined by the international border with Saudi Arabia to the north, Yemen to the west, the Al-Wusta area to the east, and the Dhofar mountain chain to the south, which separates it from the coast of the Arabian Sea, located 30 km offshore. The region spans from latitudes 17°10′00″N to 20°00′00″N and longitudes 52°00′00″E to 56°30′00″E (Figure 1). The Najd region is not densely populated due to its arid and semi-arid climate, with a small population that is primarily engaged in traditional forms of agriculture and herding; this demographic aspect emphasizes the importance of studying agricultural drought in the region, as the local population depends heavily on the limited agricultural opportunities available. The Najd region is a significant area with its own unique environmental and agricultural characteristics, and agriculture is a key component of the local economy. Therefore, the agricultural drought in this region can severely impact crop yields and livestock, leading to economic losses and affecting food security. Studying agricultural drought in this region helps in creating better water management practices to sustain agricultural productivity. The Najd region is characterized by a flat landscape with major wadis (valleys), small hills, and sand dunes, especially at the northern edge of the Ruba Al-Khali desert [23]. The elevation in the area varies from around 1000 m above sea level (m.a.s.l.) on the crest of the Jabal chain to less than 94 m.a.s.l. on the flat land surface. The Najd desert is composed of a stony plain with alluvial deposits concentrated in the main wadi channels and sand dunes [24]. The region falls within arid to semi-arid zones and is classified as one of the most arid zones globally due to high temperatures, evaporation rates, and low rainfall. Based on the Koppen–Geiger climate classification scheme [25], monthly minimum and maximum temperatures range from 11.9 °C to 42.1 °C. The highest temperatures are typically experienced from May to July, while the lowest temperatures occur between December and February annually. The average annual evaporation is 157.26 mm, with the maximum average evaporation happening from April to June and the minimum from December to February. The average relative humidity ranges from 4.1% to 92.6%, with an annual mean of 51.02%. The lowest humidity levels are usually observed in March, April, May, and October, while the highest occur in July and August. Rainfall in the Najd region is irregular and influenced by cyclone events, with an average annual precipitation of 56.7 mm and 47.6 mm at the Marmul and Thumrait stations collected in the period spanning 2001 to 2023 (Figure 1). The highest rainfall is typically recorded in March, June, and May, while the lowest occurs in February, April, and January. Most of the monsoon rainfall flows towards the Arabian Sea rather than benefiting the Najd area, except within the Jabal chain. The rainfall in this region is often light showers or drizzles and does not commonly result in significant runoff. The rainy season from November to January contributed to 46% of annual precipitation, while the dry season from June to August contributed only 16.3%. The thickness of the alluvial deposits in the area is generally thin, ranging from 0–4 m, except in some main wadi deposits [26].

2.2. The Data Used and Processing

MODIS sensor data, which is onboard the Terra and Aqua satellites operated by NASA, was used in this study. Twenty-three MODIS land products were downloaded from 2001 to 2023, with a total of three tiles to analyze and monitor environmental conditions in the study area (http://search.earthdata.nasa.gov/search, accessed on 16 March 2024). MODIS products are essential for studying agricultural drought because they offer frequent, different-resolution data on vegetation health and surface conditions; their wide spectral range enables detailed analysis, while the historical data since 2001 helps track long-term

drought patterns. MODIS's accessibility and cost-effectiveness make it a valuable tool for timely and effective drought monitoring and mitigation [27]. MODIS sensors stand out in remote sensing for agricultural drought monitoring due to their frequent near-daily global coverage (based on the instruments' orbital cycle), which surpasses the temporal resolution of both Landsat-8 and Sentinel-2, which provide coverage every 16 days and 5 days, respectively. While MODIS has a moderate spatial resolution (250 m to 1 km), less detailed than Landsat-8 (30 m) and Sentinel-2 (10 m to 60 m), it compensates with a broader spectral range of 36 bands, compared to Landsat-8's 11 bands and Sentinel-2's 13 bands. Additionally, MODIS has been operational since 2001, offering a longer continuous dataset for long-term trend analysis, whereas Sentinel-2 began in 2015, and Landsat-8 was launched in 2013. MODIS images undergo several corrections to ensure data accuracy and reliability, including radiometric correction to adjust sensor biases, geometric correction to align with geographic coordinates, and atmospheric correction to remove interference from aerosols and gases. Cloud masking is used to eliminate cloud-covered pixels, while the bidirectional reflectance distribution function (BRDF) correction adjusts for variations in reflectance due to sunlight and sensor angles. Regular calibration ensures long-term measurement accuracy; these corrections make MODIS data precise and dependable for applications such as agricultural drought monitoring [28]. In this study, MODIS/006/MOD11A2 daytime land surface temperature (LST) product data with an 8-day time resolution and 1 km spatial resolution were utilized for calculating the TCI. Additionally, NDVI data from MODIS/061/MOD13A2 and MODIS/006/MYD13A2 products were used, which have a time resolution of 16 days and a spatial resolution of 1 km. The NDVI data were pre-processed and synthesized into monthly data using the maximum value method to calculate the VCI index, and the time series analysis for that specific location was performed using the GEE platform.

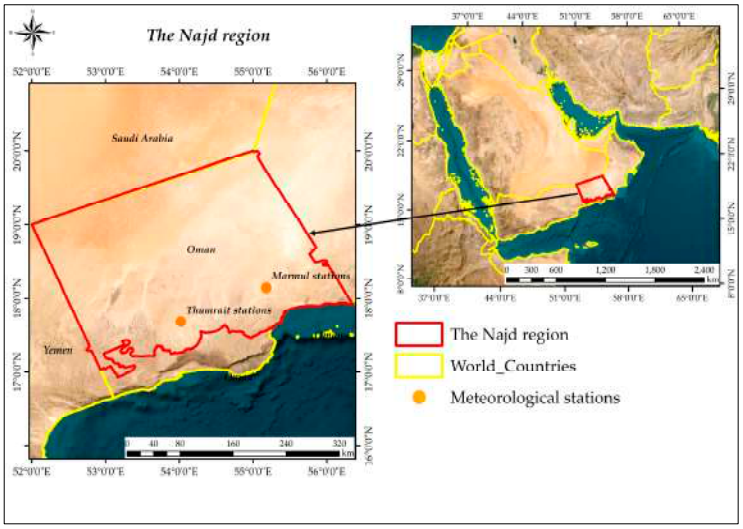

Figure 1. Geographical location of the study area (The Najd region, Sultanate of Oman).

2.3. Drought Indices (DIs) Utilization

Remote sensing (RS) has significantly advanced the ability to monitor and evaluate agricultural drought conditions and has recently emerged as a reliable and effective method of collecting data over wide areas. Several DIs have been developed and utilized, each with unique features and applications. Among these, the normalized difference vegetation index (NDVI), TCI, VCI, and VHI indices are prominent. Below is a detailed discussion of these indices, focusing on TCI, VCI, and VHI, which are particularly noted for their role in describing vegetation conditions and classifying drought severity. DI values were classified into 5 classes, extreme drought (<10), severe drought (10–20), moderate drought (20–30), mild drought (30–40), and no drought (>40) [29], as shown in Table 1.

Table 1. Drought index (DI) values and classes (after Du et al. (2013) [30]).

TCI/VCI/VHI Values	Drought Class
0 to 10	Extreme drought
10 to 20	Severe drought
20 to 30	Moderate drought
30 to 40	Mild drought
More than 40	No drought

2.3.1. Temperature Condition Index (TCI)

TCI is designed to reflect thermal conditions affecting vegetation and takes into consideration that during drought periods, there is a reduction in soil moisture, which leads to an increase in land surface temperature (LST) stress compared to normal conditions. TCI is calculated using Equation (1) [31]:

$$TCI = 100 * \left(\frac{(LSTmax - Ti)}{(LSTmax - LSTmin)} \right) \quad (1)$$

where Ti is the current temperature, $LSTmax$ is the maximum temperature over a given period, and $LSTmin$ is the minimum temperature. TCI values ranged from 0 to 100, with lower values indicating higher stress due to elevated temperatures. TCI is particularly useful in assessing drought impact, as temperature anomalies can significantly stress vegetation.

Kogan, (1997) [32] proposed a two-channel algorithm of MODIS satellite images with separate terms for the atmospheric LST. In this study, this algorithm can be written as, Equation (2):

$$LST = T_i^0 + a_1\left(T_i^0 - T_j^0\right) + a_2(1 - \varepsilon_1) + a_3\Delta\varepsilon_1 + a_4W(1 - \varepsilon_1) + a_5W\Delta\varepsilon_1 + a_0 \quad (2)$$

where ${T_i}^0$ and ${T_j}^0$ are the brightness temperatures measured at the top of the lower-layer atmosphere in MODIS satellite images tow-channel i and j; ε_1 is the channel emissivity; $\Delta\varepsilon_1$ is the difference of emissivity; W is the total water vapor content; and a_i (i = 0–5) is the channels algorithm numerical coefficient.

2.3.2. Vegetation Condition Index (VCI)

VCI utilizes NDVI to assess the relative health of vegetation by comparing current NDVI values to historical records [33]. VCI is calculated as the following Equation (3):

$$VCI = \left(\frac{NDVI - NDVImin}{NDVImax - NDVImin} \right) 100 \quad (3)$$

where $NDVImin$ and $NDVImax$ are the historical minimum and maximum of NDVI values, respectively. Values of the VCI index ranged from 0 to 100, with higher values indicating better vegetation conditions. VCI effectively normalizes NDVI, making it a robust indicator for drought assessment by identifying deviations from normal vegetation conditions.

2.3.3. Vegetation Health Index (VHI)

VCI and TCI indices were combined to represent vegetation condition through the VHI index through advanced data processing, including correlation testing of LST and NDVI as influencing factors, and a strong LST-NDVI correlation was the VHI values basis determining. The VHI index formula is shown as the following Equation (4) [34]:

$$VHI = \alpha * VCI + (1 - \alpha)TCI \quad (4)$$

The VHI formula is the combination of VCI and TCI that has a constant α of 0.5 and VHI values ranging from 0 to 100, with lower values indicating poor vegetation health and higher values signifying good health.

2.4. Pearson Correlation Coefficient Analysis (PCA)

In the Najd region from 2001 to 2023, the study evaluated the linear relationships between DIs at different time scales using the Pearson correlation analysis (PCA). The Pearson correlation coefficient measures the strength and direction of the linear relationship between two variables, x and y. A value of $r = 1$ denotes a perfect positive linear correlation, meaning that as x increases, y increases proportionally in a perfectly linear manner. Conversely, $r = -1$ indicates a perfect negative linear correlation, where y decreases proportionally as x increases. A value of $r = 0$ signifies no linear correlation, implying that there is no predictable linear relationship between x and y [35]. The sample correlation coefficient between the two variables can be computed as follows, Equation (5):

$$r_{xy} = \frac{\mathrm{cov}(x, y)}{\sqrt{\mathrm{var}(x)}\sqrt{\mathrm{var}(y)}} \quad (5)$$

where cov(x, y) is the sample covariance of x and y; var(x) is the sample variance of (x) and var(y) is the sample variance of (y).

2.5. The Drought Hazard Index (DHI) Calculation

DHI is a composite index that integrates various indicators to provide a single measure of drought risk and severity. While the exact equation for the DHI can vary depending on the methodology and the specific indicators used, a general approach involves the normalization and weighting of individual indicators [36]. The DHI index was calculated using the following Equation (6).

$$DHI = (VHIw * VHInorm) + (VCIw * VCInorm) + (TCIw * TCInorm) \quad (6)$$

where w are weights assigned based on the importance of each DI, *norm* are near-normal ratings assigned to DIs. DHI can have a value between a minimum of 10 and a maximum of 40. Table 2 shows weights and ratings assigned to drought severity. Since different drought severity levels have varying significance in assessing drought risk in the region, it is necessary to determine the impact of each drought category. The DHI index was categorized into four weights, where a weight of 1 was given for a normal drought, and a weight of 4 was given for a very severe drought, as it causes the greatest hazard [37].

Table 2. Weight and rate assigned to drought category (after Sönmez et al. (2005) [38]).

Severity	Weight	Occurrence Probability (%)	Rate
Near-normal drought	1	≥67.49	1
		67.49–68.67	2
		68.67–69.71	3
		≤69.71	4
Moderate drought	2	≥8.14	1
		8.14–8.21	2
		8.21–8.27	3
		≤8.27	4
Severe drought	3	≥3.36	1
		3.36–3.99	2
		3.99–4.47	3
		≤4.47	4
Very severe drought	4	≥1.92	1
		1.92–2.24	2
		2.24–2.59	3
		≤2.59	4

2.6. Google Earth Engine (GEE) Tools

Google Earth Engine (GEE) is a powerful cloud-based platform for planetary-scale environmental data analysis. Earth Engine features a multi-petabyte, analysis-ready data catalog integrated with a high-performance, parallel computation service. This platform is accessible via an Internet-based application programming interface (API) and includes a web-based interactive development environment (IDE) for rapid prototyping and visualization of results [39].

The drought assessment system was developed using functionalities of the GEE platform to compare DI values and assess the severity of different drought types based on monthly percentage values of drought conditions, duration, severity, and intensity.

To manage and process data values based on DI results through the GEE platform, the data upload modality was established. This model converts the original DI data from binary format to "Geo TIFF" format, which is required by GEE, and creates file metadata for the resulting data. The metadata are essential for the analysis routines, allowing data filtering based on user-specified spatio-temporal information.

For bulk data uploads, the GEE batch asset manager tool (available at GEE Asset Manager GitHub) is utilized, automating the process and saving time (Figure 2). Alternatively, the GEE asset manager can be used for data uploads, but it is less efficient for large datasets as it only allows for single-image uploads at a time.

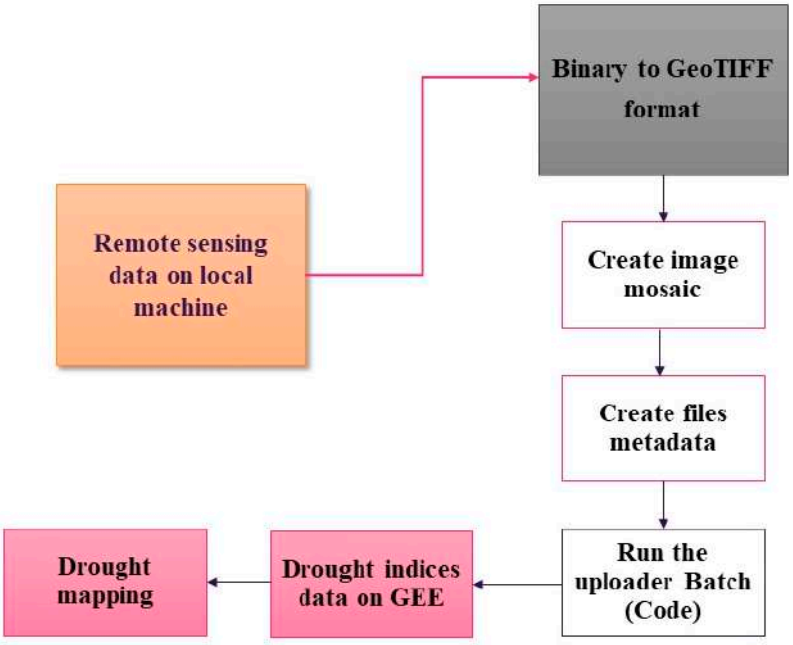

Figure 2. Schematic overview of Google Earth Engine (GEE) data processing.

2.7. The Study Methodology

Figure 3 presents the study methodology as follows: collecting meteorological data; obtaining satellite data such as imagery from platforms (e.g., National Aeronautics and Space Administration (NASA)); utilizing drought indices, such as VCI, TCI, and VHI, to assess agricultural drought conditions over time; employing GEE, a cloud-based platform for geospatial analysis to process and analyze the RS data and calculate the drought indices over the study area; investigating the relationship between DIs to understand the consistency and accuracy of the RS data in extracting drought conditions; and analyzing the results of the DIs and other data to identify and characterize the spatial distribution and severity of drought hazard in the Najd region.

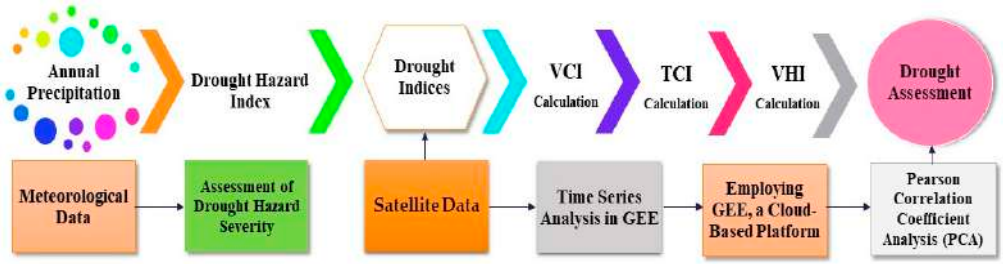

Figure 3. The methodological framework used in this study.

3. Results

3.1. Evaluation of Drought Indices

The drought indices, i.e., VCI, TCI, and VHI, are used to analyze the drought severity condition on both spatial and temporal scales from 2001 to 2023 in the Najd region, Sultanate of Oman.

3.1.1. Temperature Condition Index (TCI)

The information in Figure 9a–w provided a detailed analysis of the TCI in the Najd region over the period of 2001–2023 retrieved from MODIS satellites and the GEE platform. The TCI values exhibit variations over time, with notable minimum values observed in specific years (2001, 2005, 2009, 2010, 2014, 2015, 2016, 2017, 2019, 2020, and 2021). The TCI index time series plot in the study area experienced frequent extreme to no-drought events over the study period, and the TCI index mean values through different years ranged from 18.9 to 80.9 in the investigated area, indicating the varying severity of drought conditions over time and reflecting the dynamic nature of temperature conditions in the Najd region, as shown in Figure 4. However, the presence of occasional extreme values of the TCI index highlights the influence of local climate changes, seasonal extremes, weather anomalies, low vegetation cover, and temperature variations. This complexity underscores the dynamic and multifaceted nature of environmental conditions in the Najd region.

The TCI index trend shows an increase in temperature at the study area (based on LST values), as shown in Figure 5, leading to more severe TCI values in the years 2014 to 2023 compared to the years 2001 to 2013. Given that the Najd region is hyper-arid with high temperatures (above 45 °C) and low annual precipitation (less than 15 mm), the TCI plays a significant role in the VHI index. Whereas the TCI index is more severe in the southeast areas of the Najd area compared to the northwest areas in the years 2001, 2005, 2009, 2010, 2014, 2015, 2016, 2017, 2019, 2020, and 2021, indicating spatial variability in temperature conditions within the region.

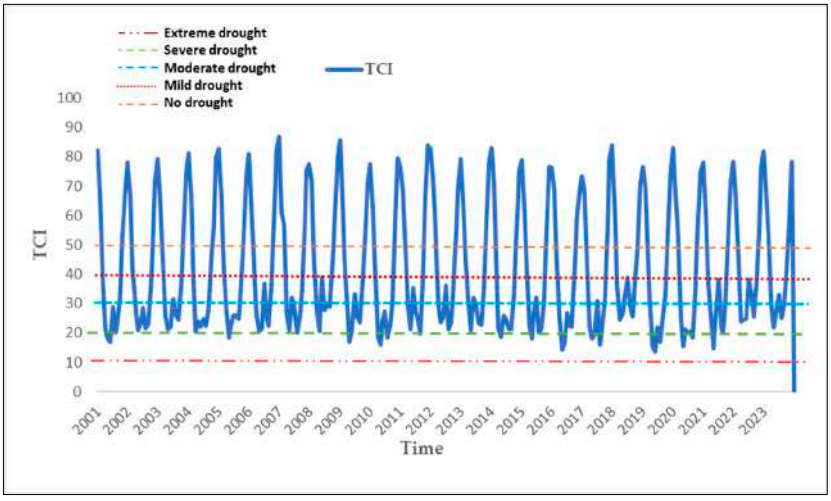

Figure 4. TCI, time series plot of the Najd region derived using GEE and MODIS images.

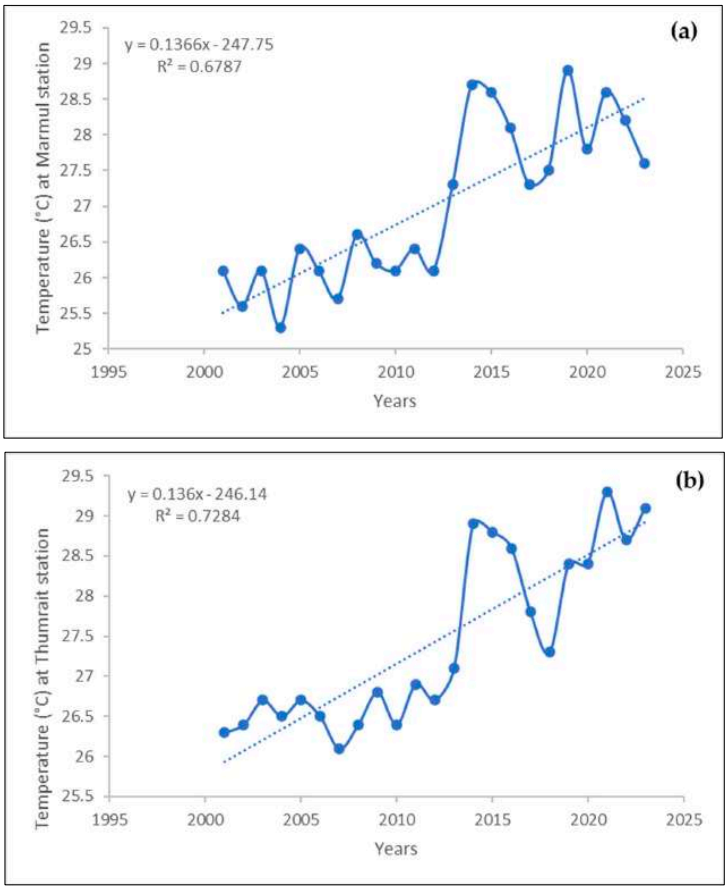

Figure 5. LST variation trends during the 2001–2023 period at (**a**) Marmul and (**b**) Thumrait meteorological stations.

3.1.2. Vegetation Condition Index (VCI)

The study conducted in the Najd region from 2001 to 2023 analyzed the VCI index derived from NDVI data to assess the spatio-temporal distribution of drought conditions, as shown in Figures 6 and 9a–w. The spatial distribution maps revealed that several years, including 2001, 2003, 2006, 2008, 2009, 2013, 2015, 2016, 2017, 2018, 2020, 2021, 2022, and 2023, were characterized by mild drought conditions. In contrast, years such as 2002, 2004, 2005, 2007, 2010, 2011, 2012, 2014, and 2019 exhibited wetter conditions with relatively no drought.

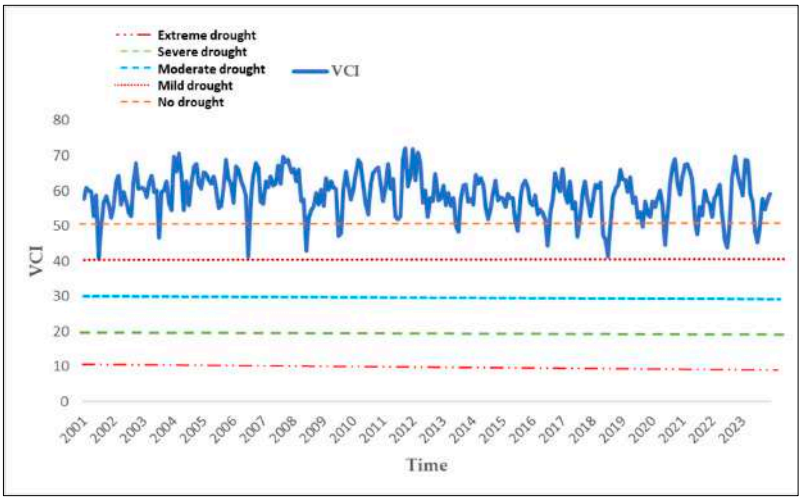

Figure 6. VCI, time series plot of the Najd region derived using GEE and MODIS images.

The time series analysis of VCI, conducted using GEE, showed that the mean VCI values ranged from 48.2 to 67 throughout the study period.

3.1.3. Vegetation Health Index (VHI)

The analysis was conducted in the Najd region using MODIS satellite imagery, and the GEE platform focused on the VHI to assess drought conditions spatially and temporally. The spatial distribution maps depicted in Figures 7 and 9a–w revealed that, with the exception of 2005 and 2007, all studied years were classified as moderate drought years across the study area. Additionally, the figures indicated that drought severity was more pronounced in the downstream region compared to the upstream region of the investigated area. The GEE-extracted VHI index time sequence chart displayed mean VHI values ranging from 36.6 to 70.5 throughout the study period. The VHI time sequence chart highlighted that the Najd region consistently experienced moderate to mild drought events in all the studied years, and in the second decade, especially in 2020, there was a notable increase in the severity and frequency of moderate drought events.

Figure 8 provides a summary of the maximum, minimum, and mean values of the TCI, VCI, and VHI indices in the Najd region on an annual period from 2001 to 2023; this figure highlights severe drought events for TCI mean values in the years 2001, 2005, 2009, 2010, 2014, 2015, 2016, 2017, 2019, 2020, and 2021. Mild drought conditions were noted based on the mean values of the VCI index in the years 2001, 2003, 2006, 2008, 2009, 2013, 2015, 2016, 2017, 2018, 2020, 2021, 2022, and 2023. In contrast, moderate drought events were noted for VHI mean values across all studied years except for 2005 and 2007.

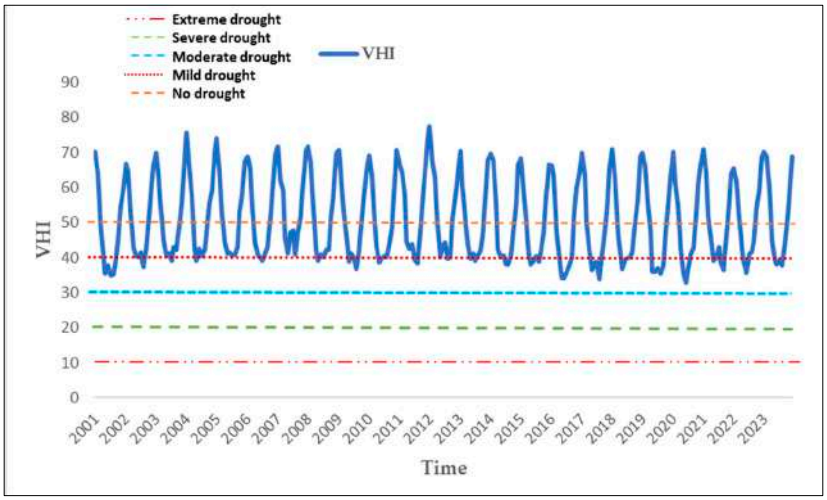

Figure 7. VHI, time series plot of the Najd region derived using GEE and MODIS images.

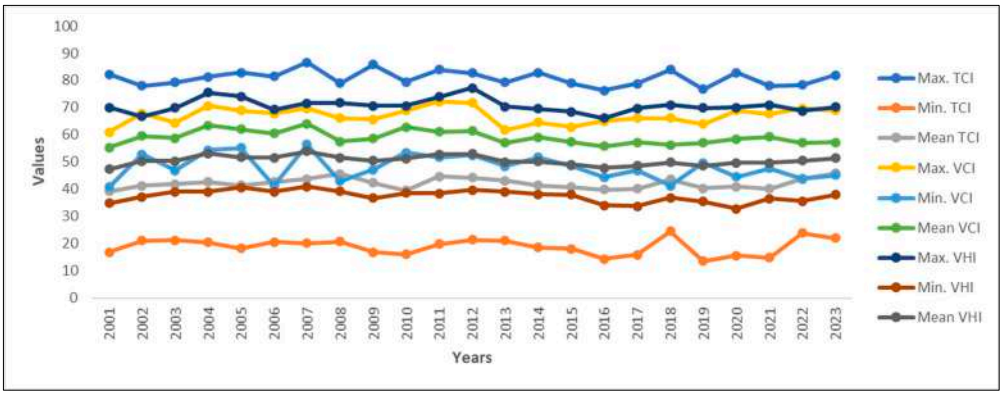

Figure 8. Descriptive statistics of VCI, TCI, and VHI values during the 2001–2023 period at the Najd region.

The concentration of values for the T TCI, VCI, and VHI between 18.7 and 80.4 indicates that the Najd region mainly experiences mild to no-drought conditions; this suggests a stable climate with moderate variations in temperature and precipitation. Additionally, the data may be averaged over larger scales, smoothing out extreme variations. Overall, these indices reflect a dynamic interaction between the relatively stable climatic conditions and the drought rate in the study area.

3.2. Pearson Correlation Coefficient Analysis (PCA) between Drought Indices (DIs)

Based on the correlation analysis between DIs (TCI, VCI, and VHI) through the study period (Table 3), the VHI index shows the highest positive correlation with the VCI index, with a correlation coefficient of 0.829 ($p < 0.01$). Furthermore, a weak correlation was observed between the VHI index and TCI index, with a correlation coefficient of 0.679. The correlation between the VCI index and TCI index was calculated, and a very weak correlation was observed (0.152).

Table 3. PCA analysis of drought indices (DIs).

	Correlation Coefficient		
	Average TCI	Average VCI	Average VHI
Average TCI	1	0.152	0.679 **
Average VCI	0.152	1	0.829 **
Average VHI	0.679 **	0.829 **	1

** Correlation is significant at the 0.01 level (2-tailed).

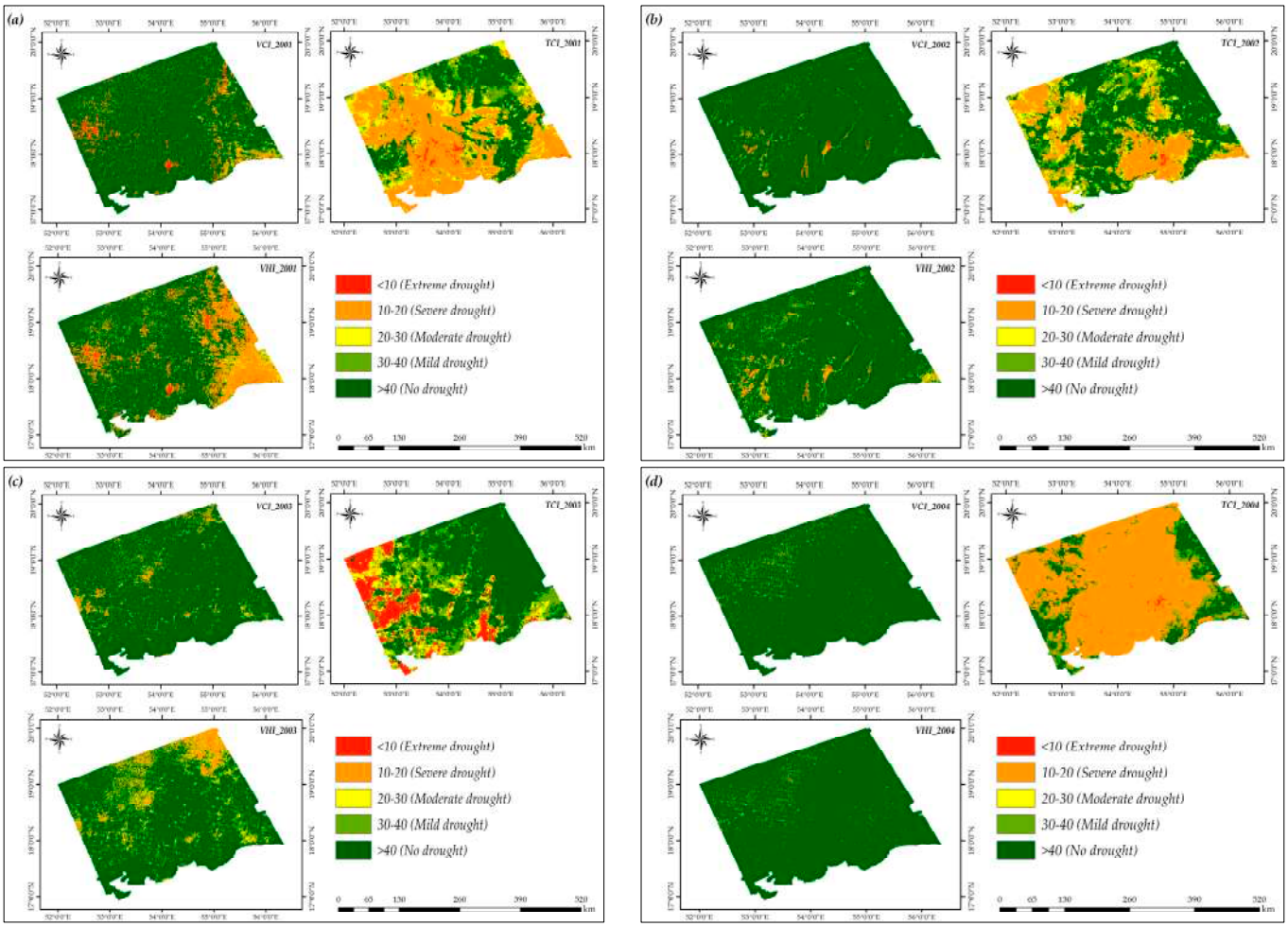

Figure 9. *Cont.*

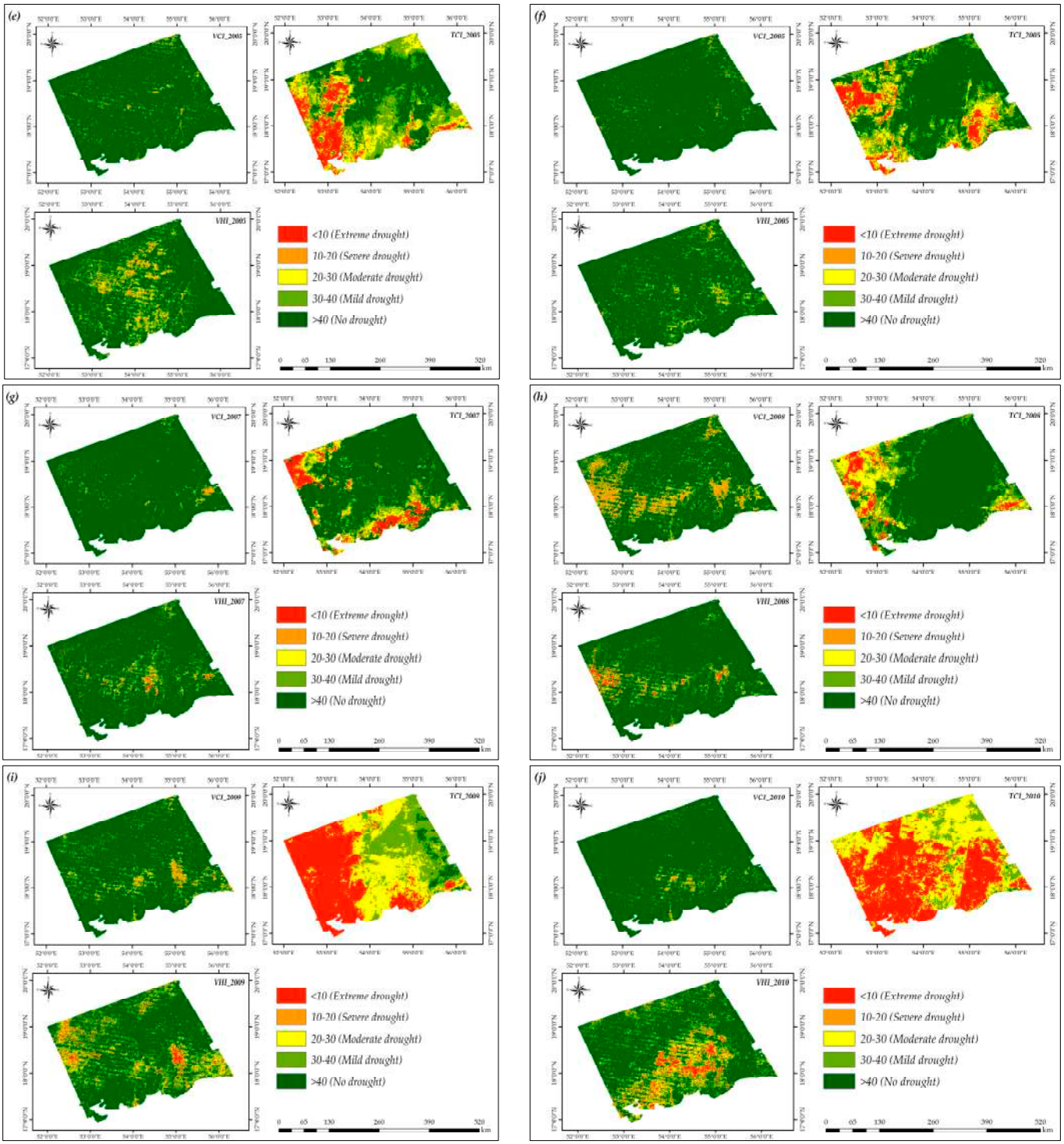

Figure 9. *Cont.*

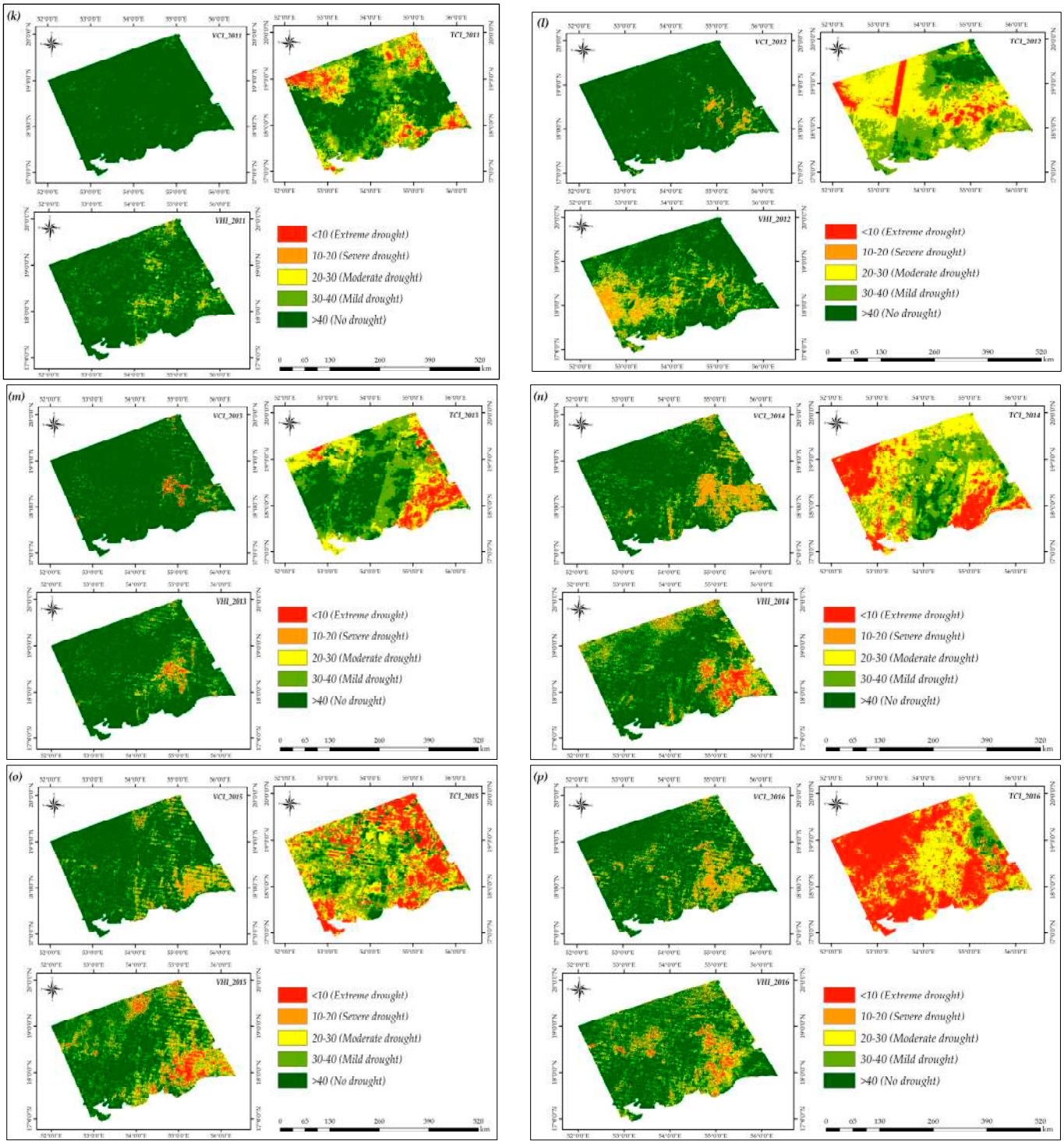

Figure 9. *Cont.*

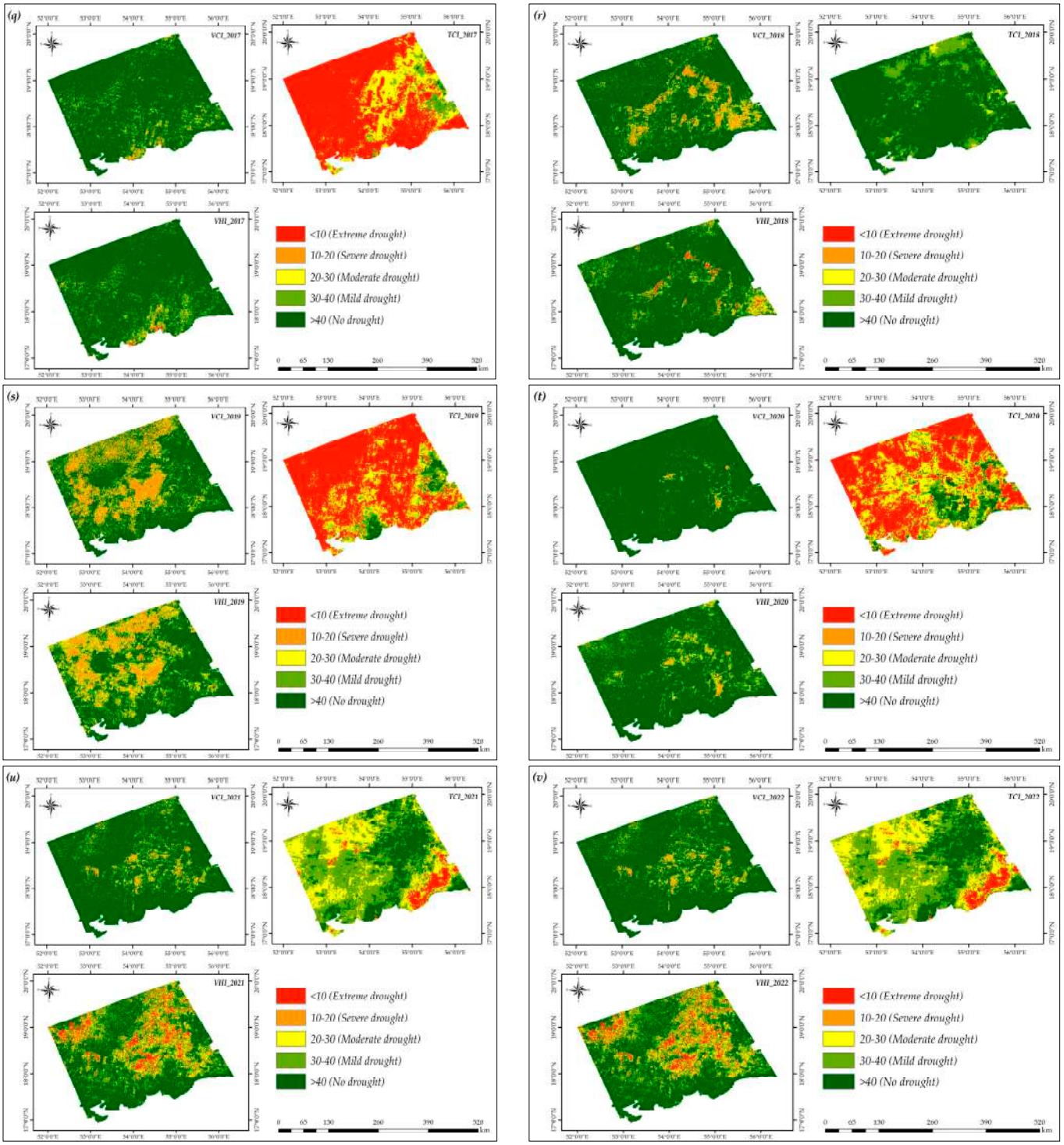

Figure 9. *Cont.*

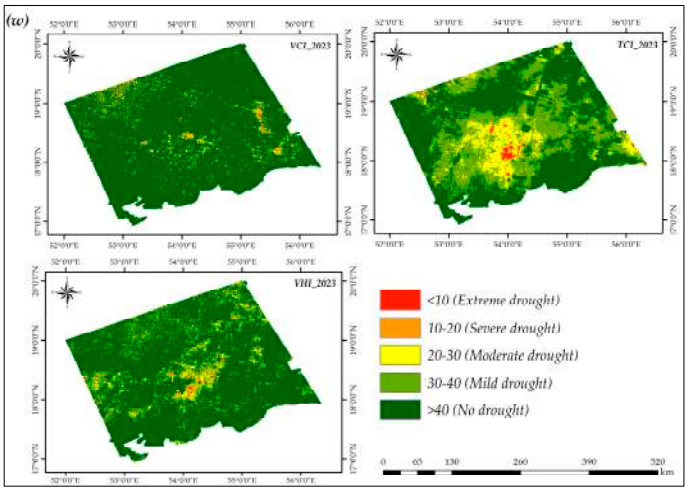

Figure 9. Spatial distribution of TCI, VCI, and VHI in the Najd region retrieved from MODIS Satellites for the period of 2001 (**a**)–2023 (**w**).

According to Table 3, the correlation between TCI, VCI, and VHI indices tends to increase with longer time periods. The vegetation growth is influenced by the current and previous months of condition, including those before vegetation growth started.

As a result, the vegetation growth regime and vegetation index are more strongly closely related to wet/drought conditions over longer time periods. This means that VHI, TCI, and VCI indices, which are closely tied to the vegetation index used to monitor the agricultural drought, show a stronger correlation over an extended period of time.

3.3. The Drought Hazard Index (DHI) Assessment

To assess the spatial distribution of drought hazard in the Najd region over a specific time period, maps of drought occurrence severity were examined. The spatial distribution of the DHI index revealed that drought hazard severity was highest in the northern parts of the study area, with a gradual decrease towards the south and eastern parts of the investigated area. It was observed that the majority of the study area experienced less than moderate drought risk, covering 44% of the total area. Additionally, a significant portion of the area (56% of the total area) was classified as having very severe drought risk, as shown in Figure 10. The percentages of areas covered by drought hazard classes at different timescales are provided in Table 4.

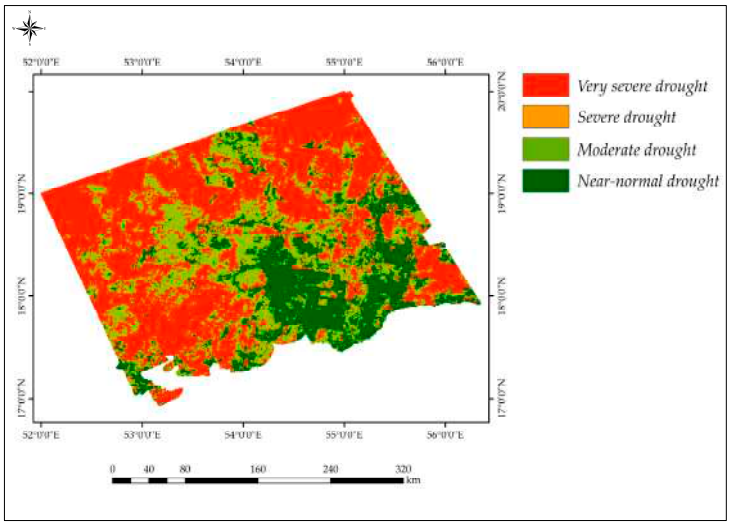

Figure 10. The spatial distribution of drought hazards in the Najd region over the time period.

Table 4. Drought hazard severity in the Najd region.

Drought Severity	Weight	Occurrence Probability (%)	Area (%)
Near-normal drought	1	≤69.71	21
Moderate drought	2	≤8.27	23
Very severe drought	4	≤2.59	56

4. Discussion

The impact of drought on agricultural productivity, climate conditions, and land desertification is indeed significant and requires thorough investigation and strategic management [40]. Therefore, this study examining multiple drought indices alongside vegetation index and surface temperature in the hyper-arid region of the Sultanate of Oman (the Najd region) from 2001 to 2023 is commendable. By considering various drought indices simultaneously, this research can provide a more comprehensive understanding of the spatiotemporal characteristics of drought in the study region [10]. Utilizing indices such as TCI, VCI, and VHI allows for a multidimensional analysis of drought impacts, considering temperature stress, vegetation health, and overall environmental conditions. This approach aligns with relevant literature, which emphasizes the importance of integrating multiple indicators to effectively capture the complexity of drought phenomena. For instance, studies such as Kogan (1997) [32] and Cao et al. (2021) [41] demonstrate that using combined indices offers a nuanced view of drought severity and its effects on ecosystems. Hence, this approach allows for a holistic view of drought conditions, which is crucial for enhancing the accuracy and reliability of drought assessment and contributing valuable insights for better drought management and mitigation strategies [42].

This study addresses a crucial aspect of environmental monitoring in regions such as the Najd region of the Sultanate of Oman, where climate change and its impacts, such as drought, are becoming increasingly severe [23]. The evaluation and correlation of DIs such as TCI, VCI, and VHI from 2001 to 2023, using data from the MODIS satellite datasets and the GEE platform, is a significant effort to enhance the accuracy and reliability of drought assessment [43]. By leveraging the extensive temporal and spatial coverage of MODIS data along with the powerful processing capabilities of GEE, this approach allows for a comprehensive analysis of drought conditions over time. This integration improves the precision of drought monitoring and provides valuable insights into the spatiotemporal dynamics of drought [44].

One of the primary challenges in agricultural drought assessment in the Sultanate of Oman is the scarcity of reliable in-situ climate data [10,45]. The sparse distribution of weather stations and the incomplete and intermittent nature of the data they provide make it difficult to capture accurate climate variations, especially temperature changes, which are critical for drought analysis [46]. Limited spatial coverage and data gaps hinder the ability to monitor and assess drought conditions comprehensively. This challenge underscores the importance of using remote sensing technologies and satellite datasets, such as those provided by MODIS, which offer consistent, wide-ranging, and continuous data. These tools can supplement ground-based observations, providing a more reliable and detailed understanding of climate dynamics and their impact on drought [47]. The use of RS data helps to mitigate these issues by providing consistent and comprehensive coverage over large areas, making it possible to monitor drought conditions more effectively and accurately [1].

The rising temperatures and worsening drought conditions in Oman, with about 50% of the country affected by severe and frequent drought events, highlight the urgent need for improved monitoring and assessment techniques [10]. The Najd region, having experienced moderate drought events consistently over the past 23 years, serves as a critical area for this study. Accurately estimating the severity and progression of droughts using

DIs can provide valuable insights into the trends and patterns of drought occurrences, which is essential for developing effective mitigation and adaptation strategies.

The results of our study are stated below:

1. The results of the TCI index values over the study period exhibit variations over time, with notable minimum observed values in specific years (2001, 2005, 2009, 2010, 2014, 2015, 2016, 2017, 2019, 2020, and 2021); this indicates periods of more severe temperature conditions in the study area during those years [14]. The TCI index values trend shows an increase in temperature in the years 2014 to 2023 compared to the years 2001 to 2013; this trend suggests a worsening of temperature conditions over the years, which can have implications for the study region's environment and ecosystems [48]. The TCI mean values throughout different years ranged from 18.9 to 80.9, indicating the varying severity of drought conditions over time. Therefore, the analysis provides valuable insights into the impact of temperature conditions on drought dynamics in the Najd region, emphasizing the importance of considering multiple factors in assessing drought conditions through indices such as TCI and VCI indices [49]. Song et al. (2018) [50] used MODIS-based indices to study drought conditions in China. Their findings highlighted how extreme temperature conditions, reflected by low TCI values, were crucial for understanding drought dynamics and impacts on agriculture. This supports the observation that minimum TCI values signify critical temperature stress periods.
2. The spatial distribution maps of the VCI index revealed that several years, including 2001, 2003, 2006, 2008, 2009, 2013, 2015, 2016, 2017, 2018, 2020, 2021, 2022, and 2023, were characterized by mild drought conditions, and the mean VCI values ranged from 48.2 to 67 throughout the study period. This indicates fluctuations in vegetation health and moisture availability in the region over the years. The results suggest a varying pattern of drought severity, with certain years experiencing milder drought conditions while others show wetter conditions. These results provide valuable insights into the dynamics of vegetation response to environmental conditions in the Najd region over the studied time period; the results are similar to the VCI analysis on spatiotemporal variations of spring drought in China by Liang et al. (2021) [51]. Omondi, (2010) [52] employed statistical models to analyze VCI trends in the Horn of Africa, finding that VCI values significantly correlated with seasonal rainfall patterns. Their analysis revealed a mean VCI decrease during drought years, with VCI values dropping by up to 20 compared to non-drought years; the study highlighted those periods with a VCI below 50 corresponded with severe drought conditions and reduced vegetation health.
3. According to VHI index spatial distribution maps, all studied years (with the exception of 2005 and 2007) were classified as moderate drought years, and the mean VHI values ranged from 36.6 to 70.5 throughout the study period. Based on Jalayer et al. (2023) [53], the VHI index results underscore the persistent nature of drought conditions in the Najd region, with a noticeable escalation in severe drought events in the latter years of the study period. The spatial and temporal analysis of VHI provides valuable insights into the evolving drought patterns in the region, emphasizing the need for effective mitigation and adaptation strategies to address the heightened risk of drought in the study area [54].
4. The high positive correlation between VHI and VCI (0.829, $p < 0.01$) underscores a robust linear relationship, implying that VCI is a significant predictor of VHI. The correlation coefficient between the VHI index and TCI index is 0.679, indicating a positive correlation. This suggests that as the VHI index increases, the TCI index tends to increase. Meanwhile, the correlation coefficient between the VCI index and TCI index is 0.152, indicating a positive and very weak correlation; this result is compatible with Al-Kindi et al.'s (2022) study [55], which aimed at drought monitoring using various drought indices (DIs) in the northern part of the United Arab Emirates.
5. The DHI index's spatial analysis reveals significant regional disparities in drought severity, highlighting the most severe conditions in the northern regions of the study

area, and the spatial distribution maps indicate that the northern regions experienced the highest levels of drought risk, with severity gradually decreasing towards the south and east. Specifically, the data show that approximately 44% of the total area fell under moderate drought risk, while a substantial 56% faced very severe drought risk. The differential in drought severity underscores the importance of understanding regional variations in drought severity and the need for proactive measures to build resilience and mitigate the impacts of drought on vulnerable communities and ecosystems [56].

Despite the advancements in satellite-based drought indices (DIs), several limitations persist; for instance, (i) ground validation is still required to ensure accuracy in local conditions, a process that is particularly challenging in remote and arid regions; (ii) the need for expertise in remote sensing and climate science means that misinterpretation of satellite-derived indices can lead to incorrect assessments of drought severity; (iii) the relatively recent introduction of continuous satellite observations (e.g., MODIS since 2001) limit the availability of long-term historical data for robust trend analysis; (iv) the moderate resolution of satellite imagery may not capture fine-scale variations in drought conditions, especially in heterogeneous landscapes or small-scale agricultural plots. Researchers in developing regions or those with limited resources may face difficulties accessing and processing large datasets, such as those available through Google Earth Engine (GEE). Furthermore, while these indices offer valuable quantitative measures, they may not fully reflect the socio-economic impacts of drought on local communities, which are essential for comprehensive risk assessment and management.

5. Conclusions and Recommendations

Conducting a comprehensive study on agricultural drought assessment in the hyper-arid region of the Sultanate of Oman using DIs (VCI, TCI, and VHI), MODIS satellite datasets, and the GEE platform is a valuable approach for monitoring and analyzing drought conditions and calculating the SAI to determine anomalies in the DIs can provide insights into the severity and duration of drought, events in the Najd region. Additionally, correlating the DIs with each other using the Pearson correlation coefficient can help identify relationships and patterns in the data. Given the limited availability of in-situ weather stations in the Najd region, RS data have become especially important for monitoring and analyzing droughts over an extended period from 2001 to 2023. This study contributes valuable information for understanding the spatial and temporal distribution of agricultural droughts in this hyper-arid region, and the study conclusions are as follows:

1. The TCI index exhibited temporal variations over the study period, with notable minimum values observed in specific years (2001, 2005, 2009, 2010, 2014, 2015, 2016, 2017, 2019, 2020, and 2021). Furthermore, there was a discernible trend of increasing temperatures from 2014 to 2023 compared to earlier years, indicating potential climate change impacts.
2. Several years, including 2001, 2003, 2006, 2008, 2009, 2013, 2015, 2016, 2017, 2018, 2020, 2021, 2022, and 2023, were characterized by mild drought conditions based on the VCI index, with mean values ranging from 48.2 to 67 throughout the study period. This suggests periodic but relatively moderate levels of vegetation stress in the region.
3. Except for 2005 and 2007, all studied years were classified as moderate drought years based on the VHI index, indicating persistent drought conditions in the region. A noticeable escalation in severe drought events was observed towards the latter years of the study period, emphasizing the evolving nature of drought patterns and the need for effective mitigation and adaptation strategies.
4. A strong positive correlation was found between VHI and VCI indices, indicating a robust linear relationship and highlighting VCI as a significant predictor of VHI. Positive correlations were also observed between VHI and TCI indices, albeit with varying strengths, while the correlation between VCI and TCI indices was positive but very weak.

5. The northern regions of the study area faced the most severe drought hazards, gradually diminishing towards the south and east. Approximately 44% of the total area was classified as under moderate drought risk, while the remaining 56% faced very severe drought risk, underscoring the widespread and significant impacts of drought in the study area.

Overall, these results emphasize the complex interplay of climatic factors and their implications for agricultural drought vulnerability in the Najd region.

In our future studies, addressing the limitations of satellite-based drought indices (DIs) involves a multifaceted approach, as follows:

1. Ground Validation and Local Accuracy:
   (a) Increase the number and coverage of ground-based monitoring stations, especially in remote and arid regions. Collaborative networks between local governments, research institutions, and international organizations can help achieve these goals.
   (b) Leverage local knowledge and observations from communities to validate satellite data and improve local accuracy.
2. Expertise and Interpretation:
   (a) Provide training for local experts and stakeholders in remote sensing and climate science to improve the interpretation of satellite data.
   (b) Develop more intuitive tools and platforms that can assist non-experts in interpreting satellite-derived indices.
3. Historical Data Limitations:
   (a) Combine satellite data with other historical datasets, such as meteorological records or historical maps, to extend the temporal analysis.
   (b) Use climate models to simulate past conditions and fill gaps in the historical record.
4. Resolution and Fine-Scale Variations:
   (a) Where possible, use higher-resolution satellite data or combine multiple data sources to capture finer-scale variations.
   (b) Apply statistical and machine learning techniques to downscale coarse-resolution data to better reflect local conditions.
5. Access to Data and Resources:
   (a) Foster partnerships between researchers, governments, and organizations to share resources and expertise.
   (b) Support and utilize open access platforms and initiatives like Google Earth Engine (GEE) to facilitate data access and processing.
6. Socio-Economic Impact Assessment:
   (a) Combine satellite data with socio-economic data through integrated assessment models to capture the broader impacts of drought.
   (b) Engage with local communities to understand and incorporate their experiences and impacts into drought assessments.

By addressing these limitations with targeted strategies, the effectiveness and reliability of satellite-based drought indices for better drought monitoring and management can be improved.

Author Contributions: Conceptualization, M.S.A.N., P.D., C.F., A.S., E.M.S. and M.E.F.; methodology, M.S.A.N., P.D., C.F., A.S., E.M.S. and M.E.F.; software, M.E.F.; validation, M.S.A.N., C.F., A.S., E.M.S. and M.E.F.; formal analysis, M.S.A.N. and M.E.F.; investigation, M.S.A.N.; resources, M.S.A.N., P.D., C.F., A.S., E.M.S. and M.E.F.; data curation, M.S.A.N., P.D., C.F., A.S., E.M.S. and M.E.F.; writing—original draft preparation, M.E.F.; writing—review and editing, M.S.A.N., P.D., C.F., A.S., E.M.S. and M.E.F.; visualization, M.S.A.N., P.D., C.F., A.S., E.M.S. and M.E.F.; supervision, M.S.A.N., C.F., A.S. and M.E.F.; project administration, C.F. and M.E.F.; funding acquisition, M.S.A.N., P.D., A.S., E.M.S. and M.E.F. All authors have read and agreed to the published version of the manuscript.

Funding: This research received no external funding.

Data Availability Statement: Data are contained within the article.

Acknowledgments: The manuscript presented a scientific collaboration between scientific institutions in three countries (Oman, Italy, and Egypt). The authors would like to thank the National Authority for Remote Sensing and Space Science (NARSS), Assiut University, University of Basilicata, and the Ministry of Agriculture, Fisheries and Water Resources of Oman for funding the field survey and satellite data.

Conflicts of Interest: The authors declare no conflicts of interest.

References

1. El Kenawy, A.M.; Al Buloshi, A.; Al-Awadhi, T.; Al Nasiri, N.; Navarro-Serrano, F.; Alhatrushi, S.; Robaa, S.; Domínguez-Castro, F.; McCabe, M.F.; Schuwerack, P.-M. Evidence for intensification of meteorological droughts in Oman over the past four decades. *Atmos. Res.* **2020**, *246*, 105126. [CrossRef]
2. Sayers, P.; Yuanyuan, L.; Moncrieff, C.; Jianqiang, L.; Tickner, D.; Xiangyu, X.; Speed, R.; Aihua, L.; Gang, L.; Bing, Q. *Drought risk Management: A Strategic Approach*; United Nations Educational, Scientific and Cultural Organization: Paris, France, 2016; ISBN 978-92-3-1000942.
3. Zhao, M.; Huang, S.; Huang, Q.; Wang, H.; Leng, G.; Xie, Y. Assessing socio-economic drought evolution characteristics and their possible meteorological driving force. *Geomat. Nat. Hazards Risk* **2019**, *10*, 1084–1101. [CrossRef]
4. Rembold, F.; Meroni, M.; Atzberger, C.; Ham, F.; Fillol, E.; Thenkabail, P. Agricultural drought monitoring using space-derived vegetation and biophysical products: A global perspective. *Remote Sens. Handb.* **2016**, *3*, 349–365.
5. Gibson, A.J.; Verdon-Kidd, D.C.; Hancock, G.R.; Willgoose, G. Catchment-scale drought: Capturing the whole drought cycle using multiple indicators. *Hydrol. Earth Syst. Sci.* **2020**, *24*, 1985–2002. [CrossRef]
6. Wang, P.; Wu, X.; Hao, Y.; Wu, C.; Zhang, J. Is Southwest China drying or wetting? Spatiotemporal patterns and potential causes. *Theor. Appl. Climatol.* **2020**, *139*, 1–15. [CrossRef]
7. Zhang, Y.; Xia, J.; Yang, F.; She, D.; Zou, L.; Hong, S.; Wang, Q.; Yuan, F.; Song, L. Analysis of drought characteristic of Sichuan province, Southwestern China. *Water* **2023**, *15*, 1601. [CrossRef]
8. Sara Tokhi, A. Yield Assessment of Grapes in Drought Prone Areas Using Satellite Remote Sensing-Based Time-Series Datasets and Machine Learning Approach. Ph.D. Dissertation, Graduated School of Life and Environmental Sciences, University of Tsukuba, Tsukuba, Japan, 2022.
9. Alahacoon, N.; Edirisinghe, M. A comprehensive assessment of remote sensing and traditional based drought monitoring indices at global and regional scale. *Geomat. Nat. Hazards Risk* **2022**, *13*, 762–799. [CrossRef]
10. Mansour, S. Geospatial modelling of drought patterns in Oman: GIS-based and machine learning approach. *Model. Earth Syst. Environ.* **2024**, *10*, 3411–3431. [CrossRef]
11. Fiorentino, C.; D'Antonio, P.; Toscano, F.; Donvito, A.; Modugno, F. New Technique for Monitoring High Nature Value Farmland (HNVF) in Basilicata. *Sustainability* **2023**, *15*, 8377. [CrossRef]
12. Belal, A.-A.; El-Ramady, H.R.; Mohamed, E.S.; Saleh, A.M. Drought risk assessment using remote sensing and GIS techniques. *Arab. J. Geosci.* **2014**, *7*, 35–53. [CrossRef]
13. West, H.; Quinn, N.; Horswell, M. Remote sensing for drought monitoring & impact assessment: Progress, past challenges and future opportunities. *Remote Sens. Environ.* **2019**, *232*, 111291. [CrossRef]
14. Wei, W.; Zhang, J.; Zhou, L.; Xie, B.; Zhou, J.; Li, C. Comparative evaluation of drought indices for monitoring drought based on remote sensing data. *Environ. Sci. Pollut. Res.* **2021**, *28*, 20408–20425. [CrossRef] [PubMed]
15. Hedayat, H.; Kaboli, H.S. Drought risk assessment: The importance of vulnerability factors interdependencies in regional drought risk management. *Int. J. Disaster Risk Reduct.* **2024**, *100*, 104152. [CrossRef]
16. He, B.; Lü, A.; Wu, J.; Zhao, L.; Liu, M. Drought hazard assessment and spatial characteristics analysis in China. *J. Geogr. Sci.* **2011**, *21*, 235–249. [CrossRef]
17. Amani, M.; Ghorbanian, A.; Ahmadi, S.A.; Kakooei, M.; Moghimi, A.; Mirmazloumi, S.M.; Moghaddam, S.H.A.; Mahdavi, S.; Ghahremanloo, M.; Parsian, S. Google earth engine cloud computing platform for remote sensing big data applications: A comprehensive review. *IEEE J. Sel. Top. Appl. Earth Obs. Remote Sens.* **2020**, *13*, 5326–5350. [CrossRef]
18. Waleed, M.; Sajjad, M. On the emergence of geospatial cloud-based platforms for disaster risk management: A global scientometric review of Google Earth engine applications. *Int. J. Disaster Risk Reduct.* **2023**, *97*, 104056. [CrossRef]
19. Aksoy, S.; Gorucu, O.; Sertel, E. Drought monitoring using MODIS derived indices and google earth engine platform. In Proceedings of the 2019 8th International Conference on Agro-Geoinformatics (Agro-Geoinformatics), Istanbul, Turkey, 16–19 July 2019; pp. 1–6.
20. Khan, R.; Gilani, H. Global drought monitoring with big geospatial datasets using Google Earth Engine. *Environ. Sci. Pollut. Res.* **2021**, *28*, 17244–17264. [CrossRef] [PubMed]
21. Ejaz, N.; Bahrawi, J.; Alghamdi, K.M.; Rahman, K.U.; Shang, S. Drought monitoring using landsat derived indices and Google Earth engine platform: A case study from Al-Lith Watershed, Kingdom of Saudi Arabia. *Remote Sens.* **2023**, *15*, 984. [CrossRef]

22. Sazib, N.; Mladenova, I.; Bolten, J. Leveraging the Google Earth Engine for drought assessment using global soil moisture data. *Remote Sens.* **2018**, *10*, 1265. [CrossRef]
23. Al-Hashmi, H. Land Degradation in the Sultanate of Oman: Reasons and Intervention Measures. In *Combating Desertification in Asia, Africa and the Middle East: Proven Practices*; Springer: Dordrecht, The Netherlands, 2013; pp. 401–423. [CrossRef]
24. Cooper, J.P.; Zazzaro, C. The Farasan Islands, Saudi Arabia: Towards a chronology of settlement. *Arab. Archaeol. Epigr.* **2014**, *25*, 147–174. [CrossRef]
25. Beck, H.E.; Zimmermann, N.E.; McVicar, T.R.; Vergopolan, N.; Berg, A.; Wood, E.F. Present and future Köppen-Geiger climate classification maps at 1-km resolution. *Sci. Data* **2018**, *5*, 180214. [CrossRef] [PubMed]
26. Al-Mashaikhi, K. Evaluation of Groundwater Recharge in Najd Aquifers Using Hydraulics, Hydrochemical, and Isotope Evidences. Ph.D. Thesis, Friedrich Schiller University, Jena, Germany, 2011.
27. Zhang, J.; Mu, Q.; Huang, J. Assessing the remotely sensed Drought Severity Index for agricultural drought monitoring and impact analysis in North China. *Ecol. Indic.* **2016**, *63*, 296–309. [CrossRef]
28. Schaaf, C.B.; Gao, F.; Strahler, A.H.; Lucht, W.; Li, X.; Tsang, T.; Strugnell, N.C.; Zhang, X.; Jin, Y.; Muller, J.-P.; et al. First operational BRDF, albedo nadir reflectance products from MODIS. *Remote Sens. Environ.* **2002**, *83*, 135–148. [CrossRef]
29. Tucker, C.J. Red and photographic infrared linear combinations for monitoring vegetation. *Remote Sens. Environ.* **1979**, *8*, 127–150. [CrossRef]
30. Du, L.; Tian, Q.; Yu, T.; Meng, Q.; Jancso, T.; Udvardy, P.; Huang, Y. A comprehensive drought monitoring method integrating MODIS and TRMM data. *Int. J. Appl. Earth Obs. Geoinf.* **2013**, *23*, 245–253. [CrossRef]
31. Kogan, F.N. Application of vegetation index and brightness temperature for drought detection. *Adv. Space Res.* **1995**, *15*, 91–100. [CrossRef]
32. Kogan, F.N. Global drought watch from space. *Bull. Am. Meteorol. Soc.* **1997**, *78*, 621–636. [CrossRef]
33. Yagci, A.L.; Di, L.; Deng, M. The effect of corn–soybean rotation on the NDVI-based drought indicators: A case study in Iowa, USA, using Vegetation Condition Index. *GIScience Remote Sens.* **2015**, *52*, 290–314. [CrossRef]
34. Gidey, E.; Dikinya, O.; Sebego, R.; Segosebe, E.; Zenebe, A. Analysis of the long-term agricultural drought onset, cessation, duration, frequency, severity and spatial extent using Vegetation Health Index (VHI) in Raya and its environs, Northern Ethiopia. *Environ. Syst. Res.* **2018**, *7*, 13. [CrossRef]
35. Cohen, J. *Statistical Power Analysis for the Behavioral Sciences*; Routledge: London, UK, 2013. [CrossRef]
36. Wilhelmi, O.V.; Wilhite, D.A. Assessing vulnerability to agricultural drought: A Nebraska case study. *Nat. Hazards* **2002**, *25*, 37–58. [CrossRef]
37. McKee, T.B.; Doesken, N.J.; Kleist, J. The relationship of drought frequency and duration to time scales. In Proceedings of the 8th Conference on Applied Climatology, Anaheim, CA, USA, 17–22 January 1993; pp. 179–183.
38. Sönmez, F.K.; Kömüscü, A.Ü.; Erkan, A.; Turgu, E. An analysis of spatial and temporal dimension of drought vulnerability in Turkey using the standardized precipitation index. *Nat. Hazards* **2005**, *35*, 243–264. [CrossRef]
39. Gorelick, N.; Hancher, M.; Dixon, M.; Ilyushchenko, S.; Thau, D.; Moore, R. Google Earth Engine: Planetary-scale geospatial analysis for everyone. *Remote Sens. Environ.* **2017**, *202*, 18–27. [CrossRef]
40. Azadi, H.; Keramati, P.; Taheri, F.; Rafiaani, P.; Teklemariam, D.; Gebrehiwot, K.; Hosseininia, G.; Van Passel, S.; Lebailly, P.; Witlox, F. Agricultural land conversion: Reviewing drought impacts and coping strategies. *Int. J. Disaster Risk Reduct.* **2018**, *31*, 184–195. [CrossRef]
41. Cao, S.; He, Y.; Zhang, L.; Chen, Y.; Yang, W.; Yao, S.; Sun, Q. Spatiotemporal characteristics of drought and its impact on vegetation in the vegetation region of Northwest China. *Ecol. Indic.* **2021**, *133*, 108420. [CrossRef]
42. Alsafadi, K.; Al-Ansari, N.; Mokhtar, A.; Mohammed, S.; Elbeltagi, A.; Sh Sammen, S.; Bi, S. An evapotranspiration deficit-based drought index to detect variability of terrestrial carbon productivity in the Middle East. *Environ. Res. Lett.* **2022**, *17*, 014051. [CrossRef]
43. Zhao, X.; Xia, H.; Pan, L.; Song, H.; Niu, W.; Wang, R.; Li, R.; Bian, X.; Guo, Y.; Qin, Y. Drought monitoring over Yellow River basin from 2003–2019 using reconstructed MODIS land surface temperature in Google Earth Engine. *Remote Sens.* **2021**, *13*, 3748. [CrossRef]
44. Hashemzadeh Ghalhari, M.; Vafakhah, M.; Damavandi, A.A. Agricultural drought assessment using vegetation indices derived from MODIS time series in Tehran Province. *Arab. J. Geosci.* **2022**, *15*, 412. [CrossRef]
45. Boluwade, A. Spatial-temporal assessment of satellite-based rainfall estimates in different precipitation regimes in water-scarce and data-sparse regions. *Atmosphere* **2020**, *11*, 901. [CrossRef]
46. Gyaneshwar, A.; Mishra, A.; Chadha, U.; Raj Vincent, P.D.; Rajinikanth, V.; Pattukandan Ganapathy, G.; Srinivasan, K. A contemporary review on deep learning models for drought prediction. *Sustainability* **2023**, *15*, 6160. [CrossRef]
47. Wu, D.; Qu, J.J.; Hao, X. Agricultural drought monitoring using MODIS-based drought indices over the USA Corn Belt. *Int. J. Remote Sens.* **2015**, *36*, 5403–5425. [CrossRef]
48. Liu, Q.; Zhang, S.; Zhang, H.; Bai, Y.; Zhang, J. Monitoring drought using composite drought indices based on remote sensing. *Sci. Total Environ.* **2020**, *711*, 134585. [CrossRef] [PubMed]
49. Zhuo, W.; Huang, J.; Zhang, X.; Sun, H.; Zhu, D.; Su, W.; Zhang, C.; Liu, Z. Comparison of five drought indices for agricultural drought monitoring and impacts on winter wheat yields analysis. In Proceedings of the 2016 Fifth International Conference on Agro-Geoinformatics (Agro-Geoinformatics), Tianjin, China, 18–20 July 2016; pp. 1–6. [CrossRef]

50. Song, Y.; Fang, S.; Yang, Z.; Shen, S. Drought indices based on MODIS data compared over a maize-growing season in Songliao Plain, China. *J. Appl. Remote Sens.* **2018**, *12*, 046003. [CrossRef]
51. Liang, L.; Qiu, S.; Yan, J.; Shi, Y.; Geng, D. VCI-based analysis on spatiotemporal variations of spring drought in China. *Int. J. Environ. Res. Public Health* **2021**, *18*, 7967. [CrossRef] [PubMed]
52. Omondi, P. Agricultural drought indices in the greater horn of Africa (GHA) countries. In Proceedings of the Agricultural Drought Indices Proceedings of an Expert Meeting, Murcia, Spain, 2–4 June 2010; p. 128.
53. Jalayer, S.; Sharifi, A.; Abbasi-Moghadam, D.; Tariq, A.; Qin, S. Assessment of spatiotemporal characteristic of droughts using in situ and remote sensing-based drought indices. *IEEE J. Sel. Top. Appl. Earth Obs. Remote Sens.* **2023**, *16*, 1483–1502. [CrossRef]
54. Kumar, V.; Chu, H.-J. Spatiotemporal consistency and inconsistency of meteorological and agricultural drought identification: A case study of India. *Remote Sens. Appl. Soc. Environ.* **2024**, *33*, 101134. [CrossRef]
55. Al-Kindi, H.; Al-Ruzouq, R.; Hammouri, N.; Shanableh, A. Monitoring Drought with Various Indices in Northern Part of UAE Using Different Satellite Image. In Proceedings of the IGARSS 2022–2022 IEEE International Geoscience and Remote Sensing Symposium, Kuala Lumpur, Malaysia, 17–22 July 2022; pp. 2339–2342. [CrossRef]
56. Nasrollahi, M.; Khosravi, H.; Moghaddamnia, A.; Malekian, A.; Shahid, S. Assessment of drought risk index using drought hazard and vulnerability indices. *Arab. J. Geosci.* **2018**, *11*, 606. [CrossRef]